HHS Public Access

Author manuscript

Liver Int. Author manuscript; available in PMC 2016 April 01.

Published in final edited form as:

Liver Int. 2015 April ; 35(4): 1145–1151. doi:10.1111/liv.12507.

Liver Regeneration and Energetic Changes In Rats Following Hepatic Radiation Therapy and Hepatocyte Transplantation by ^{31}P MRSI

Charles S. Landis[1], **Hongchao Zhou**[2], **Laibin Liu**[2], **Hoby P. Hetherington**[3], and **Chandan Guha**[2]

[1]Department of Radiation Oncology, Division of Gastroenterology and Hepatology, Department of Medicine, University of Washington, Seattle, WA

[2]Department of Radiation Oncology, Albert Einstein College of Medicine, Bronx, New York

[3]Magnetic Resonance Research Center, University of Pittsburgh, Pittsburgh, PA.

Abstract

Background & Aims—Radiation induced liver damage (RILD) is a poorly understood and potentially devastating complication of hepatic radiation therapy (RT) for liver cancers. Previous work has demonstrated that hepatocyte transplantation (HT) can ameliorate RILD in rats. We hypothesized that RT inhibits generation of cellular ATP and suppresses hepatic regeneration.

Methods—To study the metabolic changes that occur in RILD with and without HT, ^{31}P MRSI data was acquired in rats treated with partial hepatectomy (PH) alone, PH with hepatic irradiation (PHRT) or PHRT with HT (PHRT+HT).

Results—Both [γ -ATP] and ATP/Pi ^{31}P MRSI signal ratio initially decreased and subsequently returned to baseline levels within 2 weeks after PH, which is consistent with other published data. Persistently reduced [γ-ATP] and ATP/Pi ^{31}P MRSI signal ratio were observed in rats up to 20 weeks after PHRT. However, progressive increases in [γ -ATP] were observed over time in the group of rats receiving PHRT+HT. Normal [γ -ATP] was observed 20 weeks after PHRT+HT (vs. PH alone), although, ATP/Pi levels did not return to normal after PHRT +HT. *Ex vivo* histologic studies were performed to confirm liver repopulation with transplanted hepatocytes and the amelioration of pathologic changes of RILD.

Conclusions—These findings suggest that 31P MRSI can be used to monitor the progress of RILD and its amelioration using transplanted hepatocytes to simultaneously restore metabolic function while replacing host hepatocytes damaged by RT.

Introduction

Radiation therapy (RT) is often used as definitive therapy, alone or in combination with chemotherapy for a variety of solid tumors, such as, head and neck, prostate and cervix. It

*To whom all communications should be addressed at Albert Einstein College of Medicine, Montefiore Medical Center, Department of Radiation Oncology, 111 East 210 Street, Bronx, NY 10467. Phone: 718-430-3550; FAX: 718-231-5064, cguhamd@gmail.com.

There is no conflict of interest to disclose.

has also been used as adjuvant therapy after surgical resection of primary tumors. However, it has limited usage in the treatment of primary or metastatic liver cancers because of the potentially lethal complication of radiation-induced liver disease (RILD) (1). The threshold dose of whole-liver irradiation before the development of RILD has been estimated to be 30 Gy (2). More recently, the corrected mean liver dose associated with a 5% risk of RILD was noted to be 37 Gy for patients with liver metastases and 32 Gy for patients with cirrhosis and hepatocellular cancer who have worse baseline liver function (3). Although partial liver tolerance to high dose liver radiation therapy (RT) has been established, the RT doses are lowered as the volume of tumor increases, thereby, limiting RT for palliation of large hepatic tumors. The diagnosis of classic RILD is made with clinical presentations of fatigue, weight gain, anicteric ascites with rise of alkaline phosphatase (1). It is difficult to distinguish RILD from underlying liver disorders using serum biochemistry and/or imaging. Although, the clinical course of RILD is self-limiting, severe cases can be lethal with no cure. Treatment is primarily supportive with use of diuretics, paracentesis and steroids. To overcome these limitations, hepatocyte transplantation (HT) has been proposed as a potential treatment for RILD (4).

In a rodent model of RILD following partial hepatectomy (PH) and hepatic RT, we demonstrated that HT ameliorated pathological manifestations of RILD with improved survival of transplanted rats (4). Transplanted hepatocytes engrafted in irradiated liver lobes, provided metabolic support and eventually replaced the irradiated hepatocytes and repopulated the host liver. Subsequently, we have established that hepatic RT, in combination with hepatotropic mitogenic stimulus, such as, PH or systemic administration of hepatocytes growth factor (HGF) can be used as a preparative regimen for HT in the amelioration of inherited metabolic disease models in rat and mouse (5-7). A particular advantage of irradiation as a preparative regimen for HT is that it can be delivered via conformal RT, thereby, spatially confining the radiation injury to a portion of the liver and thus enabling selective engraftment and repopulation of the transplanted hepatocytes only in the irradiated lobes of liver. Since partial liver irradiation can be safely administered without inducing any clinical RILD, clinical translation of partial hepatic irradiation-based preparative regimens for HT could be feasible. Towards the clinical application of RT for the treatment of liver tumors and preparative regimens for HT, we need a diagnostic test to monitor liver function following hepatic irradiation.

There are few early diagnostic markers for RILD and clinical symptoms typically appear at late stages. Hence, monitoring the success of HT for ameliorating RILD in clinical setting would prove to be challenging. There is a need for developing noninvasive imaging methods to assess hepatic radiation injury. Furthermore, such imaging techniques could be used to evaluate the efficacy of HT and monitor donor cell engraftment, repopulation and metabolic function. Multiple studies have shown that ^{31}P MRS can reliably monitor liver regeneration and energetic status following partial hepatectomy (PH) in animals (8-10) and humans (11-13). We hypothesized that *in vivo* ^{31}P MRSI would be able to quantify ATP and other phosphorylated metabolites in irradiated liver tissue, thereby, providing a glimpse of the metabolic function for monitoring RILD. In this report, we studied the metabolic changes that occur in RILD and monitored the phosphorylated metabolites in irradiated livers *in vivo*

by ^{31}P MRSI, following treatment of F344 rats with PH alone, PHRT or PHRT+HT. In addition, histopathological analyses were performed to document the pathologic changes of RILD and document liver repopulation by transplanted hepatocytes.

Materials and Methods

Animals

Male F344 rats, from Taconic Farms (German Town, NY) and congeneic dipeptidyl peptidase IV (DPPIV)-deficient (DPPIV-ve) F344 rats, from Animals Core of the Marion Bessin Liver Research Center were housed in the Institute for Animal Studies at the Albert Einstein College of Medicine and all experiments followed the guidelines outlined in the NIH Guide for the Care and Use of Laboratory Animals (revised 1985) prepared by the National Academy of Science.

Experimental Design

F344 rats were subjected to PH alone (n=7), PHRT (n=14), or PHRT +HT (n=10). The number of animals used was based on preliminary survival data which showed a 100%, 40% and 60% survival after PH, PHRT, and PHRT+HT, respectively. Animals were anesthetized by closed circuit isofluorane inhalation. Sixty-eight percent PH was performed in rats between 8 a.m. and 12 p.m., as described previously (14). A single fraction of RT (50 Gy) was delivered to the residual liver lobes, immediately following PH, using previously published protocol (4). Briefly, animals received hepatic irradiation after surgical exposure of the liver and shielding of the stomach and intestine with 2 mm lead shields. Radiation was delivered via a Philips orthovoltage unit operating at 320 kVP, 5 mA, and 0.5 mm copper filtration at 200cGy/minute. Donor hepatocytes were isolated from syngeneic F344 or congeneic DPPIV-ve F344 rat donor livers using a modified 2-step collagenase perfusion technique (15, 16). Twenty-four hours after PHRT, animals receiving PHRT+HT were anesthetized and the spleen was exposed by a left lateral subcostal incision, followed by injection of 2-4×10^6 donor hepatocytes suspended in 0.5 ml RPMI 1640 into the splenic pulp, according to published protocols (17, 18). Animals were followed for survival until 12 weeks when they were sacrificed to perform histological studies.

^{31}P MRSI Acquisition

^{1}H MRI and ^{31}P MRSI data were acquired with a 9.4 T Varian INOVA MR system using a 7cm i.d. ^{1}H linear birdcage coil and a 2.5 cm ^{31}P surface coil. Rats were intubated and anesthetized with 1.5-2% Isoflurane. MR acquisition was gated to the manual ventilation rate. The core body temperature was maintained at 36-37° during each study. For ^{31}P MRSI, a 90° adiabatic hyperbolic secant excitation pulse and 3D spherical k-space sampling scheme on a 13×13×13 grid was used (FOV=48×48×48mm, TR=1s). MRS studies were performed 1 day and 1, 2, 4, 6, and 12 weeks after PH, PHRT, or PHRT+HT (n=3-5 rats/time point).

Data Processing

For analysis, a ^{31}P MRSI voxel from the same anatomical location (162 mL, six contiguous voxels) was selected from each study (ROI shown in Figure 1). Spectra were fit and

quantified using algorithms described previously (19). ^{31}P metabolite concentrations were estimated using results from a separate a Na_3PO_4 phantom study and *in vivo* T_1 measurements to correct for partial saturation effects. To estimate T_1 of liver metabolites, a separate nonlocalized study was performed on a healthy rat. The following T_1 values were determined and used: PME = 1.6s, Pi = 1.1s, PDE = 2s, γATP = 0.5s, βATP = 0.5s, and αATP = 1.2s.

Liver Histology

Liver was embedded in tissue freezing medium, OCT and frozen in liquid nitrogen or fixed in 10% formalin for 24 hrs and paraffin embedded. Paraffin sections were stained by hematoxylin and eosin for histopathological evaluation. DPPIV histochemistry was performed on 5 μm frozen sections of tissue using standard techniques (4). For immunohistochemistry, rehydrated sections were subjected to microwave antigen retrieval using 10 mM citrate buffer followed by standard immunohistochemical procedures using anti-BrdU, anti-OV6, anti-GFP antibodies.

Statistics

Statistical analysis was performed using MATLAB and SPSS software. All data are expressed as the mean ± standard error. Statistical significance was determined using a Student t-test for comparisons between groups. Time-adjusted survival of animals was analyzed by the Kaplan-Meier method (20) and a $p<0.05$ was considered as significant difference by the log-rank test.

Results

Non-invasive monitoring of liver bioenergetics following PH using ^{31}P MRSI

^{31}P MRSI was used to monitor liver bioenergetics after PH, PHRT, and PHRT +HT. Figure 1 displays MRSI from 6 contiguous voxels from the same anatomical location of liver of a rat that received no treatment. Representative localized ^{31}P MRS spectra from a rat liver, 30 days after PH, PHRT+HT, and PHRT are displayed in Figure 2 a, b, and c respectively. The time course of estimated concentration of [γ-ATP] and the ratio of ATP/Pi (Pi, inorganic phosphate) signal for each group is displayed in Fig. 3a and 3b, respectively. Both [γ -ATP] and ATP/Pi ^{31}P MRSI signal ratio initially decreased and subsequently returned to baseline levels within 2 weeks after PH, indicating the normalization of the hepatic bioenergetics reserve and the completion of compensatory hepatic regeneration following PH.

RT inhibited hepatocyte regeneration and caused persistently reduced [γ-ATP] levels in animals receiving PHRT

Twenty-four hours after PH or PHRT, a subgroup of animals from each group received a single dose of BrdU (50mg/Kg body weight) intraperitoneally and animals were sacrificed 6 hours later. Fig 4a and 4b displays the BrdU immunohistochemistry of liver sections from rats sacrificed 1 day after PH or PHRT, respectively. Extensive BrdU incorporation was observed in animals that were treated with PH alone. RT dramatically reduced the proportion of hepatocytes with BrdU incorporation. There were a few nonparenchymal cells that were incorporating BrdU in PHRT animals. Additionally, there was persistently reduced

[γ-ATP] and ATP/Pi ^{31}P MRSI signal ratio observed in rats up to 20 weeks after PHRT, indicating the loss of hepatic ATP reserve after irradiation (Fig 2c and 3a and B).

PHRT induces RILD with extensive oval cell proliferation

There was no mortality seen after PH alone. In contrast, there was very high mortality in the PHRT group (Figure 3c), which had a median survival time of 7.4 ± 1.4 weeks and less than 25% survival after 12 weeks. Of the rats that survived between 6-12 weeks, extensive bile duct proliferation (Figure 4C and F) and intraand extra-billiary OV-6 positive oval cells (Figure 4D) were observed. The expansion of the oval cells in PHRT animals could represent an attempt by the reserve hepatic progenitor cells to proliferate and compensate for the loss of hepatic parenchyma in PHRT animals with suppressed hepatic regeneration.

HT ameliorated RILD with extensive repopulation by the transplanted hepatocytes in irradiated livers of PHRT+HT animals and restored [γ-ATP] to baseline levels by 12 weeks

There was a significant improvement in survival of animals that received HT after PHRT with a median survival time of 8.8 weeks (95% CI: 5.9 to 11.6), compared to a median survival time of 6.1 weeks (95% CI: 4.0 to 8.2) after PHRT alone. Hematoxylin and eosin staining of liver demonstrated minimal histologic changes of RILD (Fig 4E). There was no evidence of bile ductular reaction and OV-6 positive cells were scant upon immunostaining. In order to trace and histologically monitor donor cell engraftment and repopulation, we used DPPIV histochemistry for identifying donor cells. Early experiments demonstrated that whole liver irradiation was lethal in DPPIV-deficient animals that received PHRT. In order to avoid the increased hepatic radiosensitivity of DPPIV-deficient animals, we performed PHRT in wild-type DPPIV-proficient F344 rats and transplanted DPPIV-deficient hepatocytes in these animals. DPPIV enzyme histochemistry demonstrated extensive repopulation of the irradiated liver by the transplanted DPPIV-deficient hepatocytes (blue stain), 12 weeks after PHRT+HT (Fig. 4G,H). Interestingly, there was a gradual increase in [γ-ATP] in the PHRT+HT group with baseline levels observed by 12 weeks after HT (3.0±0.12 mM). Neither the PHRT (1.44±0.15) nor the PHRT+HT (1.51±0.1) groups returned to control ATP/Pi values, observed in animals treated with PH alone (1.74±0.05) at 12 weeks. Statistically significant changes in PME and PDE were not observed between groups at any time point (Fig 2 and 3a,b).

Discussion

Liver tumors are a major problem worldwide. Primary hepatocellular carcinoma is the third leading cause of cancer mortality in the world. Most primary liver tumors are unresectable upon diagnosis and chemotherapy rarely cures these patients. In many cancers, such as head and neck, esophagus, lung, cervix and rectal cancer, RT with or without chemotherapy cures primary tumor, thereby improving survival of these patients. But RT has been traditionally used in a palliative role for liver tumors because of the potential for inducing fatal RILD. Currently, there are no diagnostic tests for RILD and treatment is usually supportive.

In this study, we modeled RILD in F344 rats by administering irradiation to the liver remnants following 66% PH. PHRT induced severe RILD in these animals, as evidenced by

increased mortality and histopathological changes that included perivenous lobular collapse, bile ductular proliferation and oval cell activation followed by periportal fibrosis (Fig 4C,D and F). Oval cells have been previously identified based on OV-6 surface expression, coupled with the morphological features of ovoid nuclei, a high nucleus/cytoplasm ratio, and proximity to the canal of herring. In PHRT animals there was characteristic expansion of the oval cell compartment despite high mortality, indicating an unsuccessful attempt in liver regeneration following PHRT. However, it is clear that endogenous oval cells alone were not capable of regenerating the irradiated liver and could not ameliorate RILD and improve survival of the animals that received PHRT. This suggests that the proliferative capacity of oval cells, like those of parenchymal hepatocytes, may also be diminished by RT. Furthermore, the number of oval cells present in the adult rat liver may not be sufficient for recovery following PHRT.

In order to treat RILD by providing metabolic support to the irradiated liver, we transplanted unirradiated primary hepatocytes via intrasplenic injection, 1 day after PHRT. Transplanted hepatocytes preferentially proliferated in irradiated liver and ameliorated RILD in the PHRT animals, possibly because donor hepatocytes responded to mitotic stimuli in the resected liver while irradiated host hepatocytes were unable to regenerate (Fig 4B). Furthermore, transplanted hepatocytes provided metabolic support, as evidenced by ^{31}P MRSI studies demonstrating a gradual increase in hepatic [ATP] levels, which was absent in PHRT animals without HT.

^{31}P MRSI has been used to monitor the bioenergetics of liver post-resection in rodents non-invasively (8, 10). These studies reported that the ATP/Pi ratio was reduced within 24 hours of PH and established the significance of ATP/Pi as a reliable index of the hepatic cytosolic energy status and/or phosphorylation potential. Previous studies with invasive MRSI of liver tissues, following PH, indicated that the Pi levels increased, thereby reducing the ATP/Pi ratio after PH (21). Similar to these studies, we observed that both the [ATP] levels and the ATP/Pi ratio were reduced after PH. These values returned to baseline within 2 weeks of PH when the hepatic regeneration is completed. Thus, the ATP/Pi ratio might reflect the hepatic regeneration status in the liver.

In contrast, persistently low [ATP] and ATP/Pi were observed in PHRT animals (Fig 3), indicating that RT reduced the bioenergetic reserve and liver function, thus inducing RT-induced hepatic metabolic injury in these animals. HT restored the bioenergetic reserve and liver function over time as evidenced by the gradual normalization of [ATP] levels in irradiated host liver by MRSI and histopathological evidence of amelioration of RILD with improved survival of PHRT-HT animals. The estimated [γ-ATP] levels (3.1±0.18 mM) in these rats were indistinguishable from control animals that received PH only (3.3±0.14 mM, n=4) at 20 weeks. However, ATP/Pi signal ratio was depressed at 20 weeks in rats receiving PHRT-HT (1.43±0.17 vs. 1.65±0.04 for PH only at 20 weeks), although the difference did not reach statistical significance. This is likely due to ongoing proliferation given that donor DPPIV deficient hepatocytes constituted less than 50% of the parenchymal cells in the host liver at this time point. The ATP/Pi ratio remained depressed during the study period of 20 weeks, suggesting ongoing hepatocellular regeneration, especially proliferation of transplanted hepatocytes. The persistently reduced ATP/Pi ratio coupled with normalizing

[ATP] levels in the PHRT-HT group indicates that transplanted hepatocytes can simultaneously restore metabolic function and proliferate over time to replace host hepatocytes damaged by RT. Significant variations in the γ-ATP MRS signal were observed in the PHRT and PHRT-HT groups compared to control and PH rats at later time points. This could be attributed to regional variations in the pathological changes of RILD, which were observed in the histological studies. Spatial heterogeneity in donor hepatocyte engraftment and repopulation may also account for variations seen in the PHRT+HT group. Statistically significant changes in PME and PDE were not observed in this study. This may have been due to the relatively short TR in this study coupled with the relatively long T_1 values for these metabolites leading to low signal intensities. Previous studies reported increased PME/PDE signal ratio following PH in rats (3,4) and humans (5). However, these studies used longer repetition times and 1H decoupling, which increased the resolution sensitivity for the PME and PDE resonances.

Despite recent advances in RT treatment planning, particularly 3D-conformal RT, intensity modulated RT (IMRT), and stereotactic body radiotherapy (SBRT), with respiratory gating and image guidance, which have facilitated the safe use of radiation dose escalation in unresectable liver cancers (22-24), RILD remains a chief concern (25, 26). Our findings suggest that 31P MRSI can be used to monitor the progress of RILD and its amelioration using transplanted hepatocytes to simultaneously restore metabolic function while replacing host hepatocytes damaged by RT. In order to account for inherent variability in baseline ATP levels from patient to patient, especially in chronic liver injury, which could trigger the loss of cellular ATP of hepatocytes (27), baseline MRSI acquisition would be needed to allow for monitoring of a further decline in ATP levels following radiation therapy.

In summary, we have established a rodent model of RILD after PHRT, where RT reduces the hepatic [ATP] levels, as measured by ^{31}PMRSI, along with suppression of parenchymal hepatocellular regeneration. Transplantation of primary hepatocytes ameliorated the histopathological changes of RILD, providing metabolic support with recovery of hepatic [ATP] levels. Given the spatial heterogeneity of hepatic radiation injury in RILD and the engraftment and repopulation of transplanted hepatocytes, ^{31}PMRSI may prove to be better suited to monitor the progress of RILD and donor hepatocyte repopulation than histopathological approaches following serial biopsies.

Acknowledgments

Supported by R01 DK64670 and R21/R33 CA121051 (to CG).

Abbreviations

RILD	Radiation induced liver damage
RT	Radiation therapy
HT	Hepatocyte transplantation
PH	Partial hepatectomy

PHRT	PH with hepatic irradiation
HGF	Hepatocytes growth factor
DPPIV	Dipeptidyl peptidase IV

REFERENCES

1. LAWRENCE TS, ROBERTSON JM, ANSCHER MS, JIRTLE RL, ENSMINGER WD, FAJARDO LF. Hepatic toxicity resulting from cancer treatment. International Journal of Radiation Oncology, Biology, Physics. 1995; 31(5):1237–48.
2. JIRTLE RL, ANSCHER MS, ALATI T. Radiation sensitivity of the liver. Adv Radiat Biol. 1990; 14:269–311.
3. PAN CC, KAVANAGH BD, DAWSON LA, et al. Radiation-associated liver injury. Int J Radiat Oncol Biol Phys. 2010; 76(3 Suppl):S94–100. [PubMed: 20171524]
4. GUHA C, SHARMA A, GUPTA S, et al. Amelioration of radiation-induced liver damage in partially hepatectomized rats by hepatocyte transplantation. Cancer Res. 1999; 59(23):5871–4. [PubMed: 10606225]
5. GUHA C, PARASHAR B, DEB NJ, et al. Normal hepatocytes correct serum bilirubin after repopulation of Gunn rat liver subjected to irradiation/partial resection. Hepatology. 2002; 36(2): 354–62. [PubMed: 12143043]
6. JIANG J, SALIDO EC, GUHA C, et al. Correction of hyperoxaluria by liver repopulation with hepatocytes in a mouse model of primary hyperoxaluria type-1. Transplantation. 2008; 85(9):1253–60. [PubMed: 18475180]
7. KAWASHITA Y, GUHA C, MOITRA R, et al. Hepatic repopulation with stably transduced conditionally immortalized hepatocytes in the Gunn rat. J Hepatol. 2008; 49(1):99–106. [PubMed: 18466997]
8. KOOBY DA, ZAKIAN KL, CHALLA SN, et al. Use of phosphorous-31 nuclear magnetic resonance spectroscopy to determine safe timing of chemotherapy after hepatic resection. Cancer Res. 2000; 60(14):3800–6. [PubMed: 10919653]
9. ZAKIAN KL, D'ANGELICA M, MATEI C, et al. A quantitative assessment of liver metabolites during jaundice using three dimensional phosphorus chemical shift imaging. Magn Reson Imaging. 2000; 18(2):181–7. [PubMed: 10722978]
10. CORBIN IR, BUIST R, VOLOTOVSKYY V, PEELING J, ZHANG M, MINUK GY. Regenerative activity and liver function following partial hepatectomy in the rat using (31)P-MR spectroscopy. Hepatology. 2002; 36(2):345–53. [PubMed: 12143042]
11. MANN DV, LAM WW, HJELM NM, et al. Human liver regeneration: hepatic energy economy is less efficient when the organ is diseased. Hepatology. 2001; 34(3):557–65. [PubMed: 11526542]
12. CORBIN IR, RYNER LN, SINGH H, MINUK GY. Quantitative hepatic phosphorus-31 magnetic resonance spectroscopy in compensated and decompensated cirrhosis. Am J Physiol Gastrointest Liver Physiol. 2004; 287(2):G379–84. [PubMed: 15191882]
13. ZAKIAN KL, KOUTCHER JA, MALHOTRA S, et al. Liver regeneration in humans is characterized by significant changes in cellular phosphorus metabolism: assessment using proton-decoupled 31P-magnetic resonance spectroscopic imaging. Magn Reson Med. 2005; 54(2):264–71. [PubMed: 16032692]
14. HIGGINS GM, ANDERSON RM. Experimental pathology of the liver. Restoration of the liver of the white rat following partial surgical removal. Arch Pathol. 1931; 12:186.
15. BERRY MN, FRIEND DS. High-yield preparation of isolated rat liver parenchymal cells: a biochemical and fine structural study. J Cell Biol. 1969; 43(3):506–20. [PubMed: 4900611]
16. NEUFELD, DS. Isolation of rat hepatocytes. Humana Press Inc; Totowa, NJ: 1997.
17. BAUMGARTNER D, LAPLANTE-O'NEILL PM, SUTHERLAND DE, NAJARIAN JS. Effects of intrasplenic injection of hepatocytes, hepatocyte fragments and hepatocyte culture supernatants

on D-galactosamine-induced liver failure in rats. Eur Surg Res. 1983; 15(3):129–35. [PubMed: 6345168]

18. GUPTA S, ARAGONA E, VEMURU RP, BHARGAVA KK, BURK RD, CHOWDHURY JR. Permanent engraftment and function of hepatocytes delivered to the liver: implications for gene therapy and liver repopulation. Hepatology. 1991; 14(1):144–9. [PubMed: 2066062]
19. LANDIS CS, YAMANOUCHI K, ZHOU H, et al. Noninvasive evaluation of liver repopulation by transplanted hepatocytes using 31P MRS imaging in mice. Hepatology. 2006; 44(5):1250–8. [PubMed: 17058269]
20. KAPLAN EL, P. M. Nonparametric estimation from incomplete observations. Journal of American Statistical Association. 1958; 53:457–816.
21. CAMPBELL KA, WU YP, CHACKO VP, SITZMANN JV. In vivo 31P NMR spectroscopic changes during liver regeneration. J Surg Res. 1990; 49(3):244–7. [PubMed: 2395369]
22. BEN-JOSEF E, LAWRENCE TS. Radiotherapy for unresectable hepatic malignancies. Semin Radiat Oncol. 2005; 15(4):273–8. [PubMed: 16183481]
23. DAWSON LA, GUHA C. Hepatocellular Carcinoma: Radiation Therapy. Cancer J. 2008; 14(2): 111–16. [PubMed: 18391616]
24. TSE RV, GUHA C, DAWSON LA. Conformal radiotherapy for hepatocellular carcinoma. Crit Rev Oncol Hematol. 2008; 67(2):113–23. [PubMed: 18308583]
25. CHENG JC, WU JK, HUANG CM, et al. Radiation-induced liver disease after radiotherapy for hepatocellular carcinoma: clinical manifestation and dosimetric description. Radiother Oncol. 2002; 63(1):41–5. [PubMed: 12065102]
26. LIANG SX, ZHU XD, XU ZY, et al. Radiation-induced liver disease in three-dimensional conformal radiation therapy for primary liver carcinoma: the risk factors and hepatic radiation tolerance. Int J Radiat Oncol Biol Phys. 2006; 65(2):426–34. [PubMed: 16690430]
27. CORBIN IR, BUIST R, PEELING J, ZHANG M, UHANOVA J, MINUK GY. Hepatic 31P MRS in rat models of chronic liver disease: assessing the extent and progression of disease. Gut. 2003; 52(7):1046–53. [PubMed: 12801965]

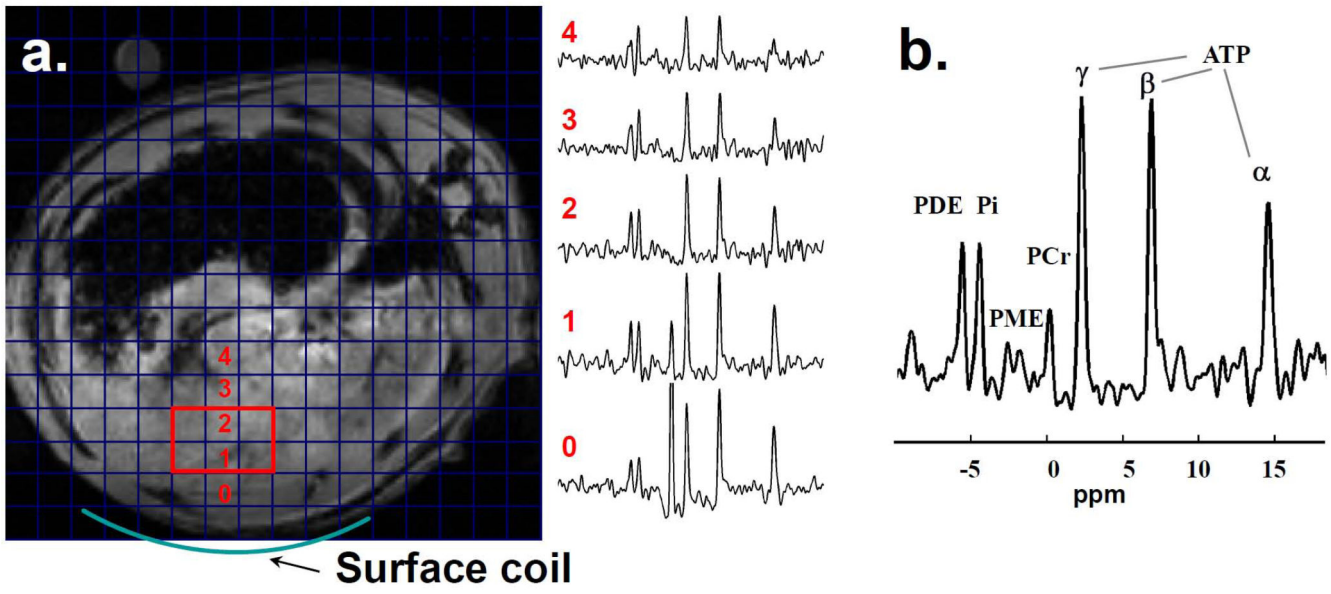

Figure 1.

Experimental setup for ^{1}H and ^{31}P MRS studies. A spin echo $^{1}H_2O$ scout image is overlaid with a grid demonstrating the ^{31}P spectroscopic image resolution. The location of the ^{31}P surface coil is indicated. ^{31}P MRS spectra from the corresponding spectroscopic imaging voxels are shown. The volume used for analysis is shown in red and the corresponding ^{31}P MRS spectrum from that volume is shown in b.

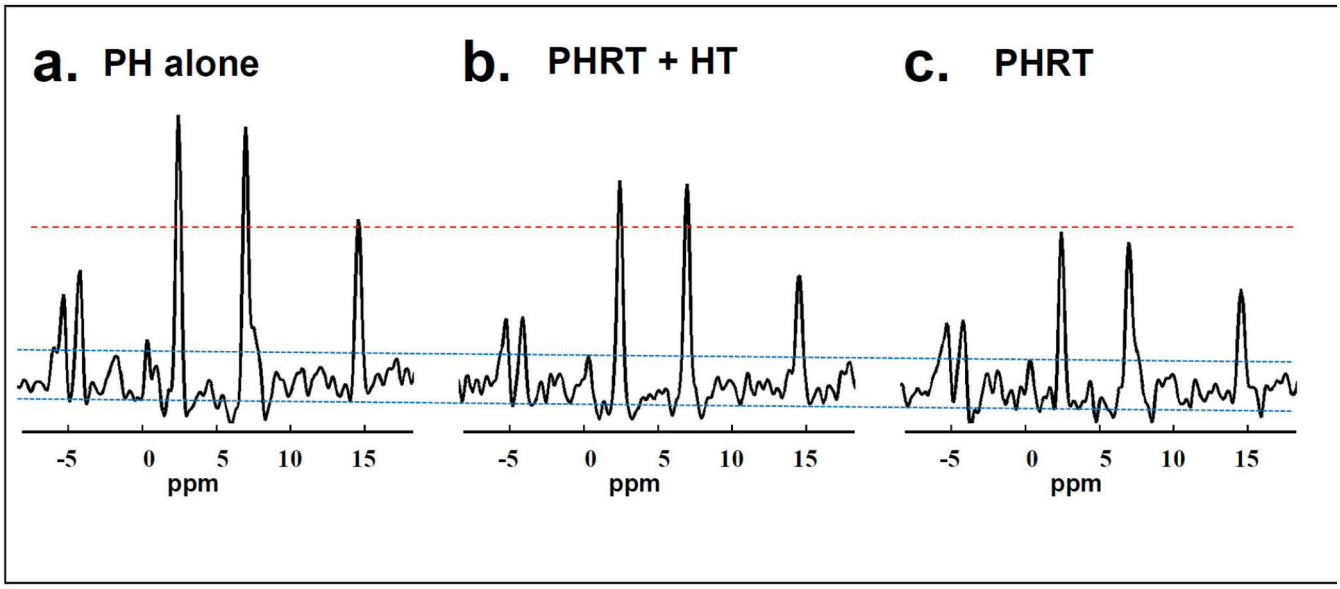

Figure 2.

Representative localized ^{31}P MRS spectra from rats. Progressively diminishing ATP signal is seen in each group 30 days after PH, PHRT+HT, and PHRT which are displayed in Figure 2 a, b, and c respectively..

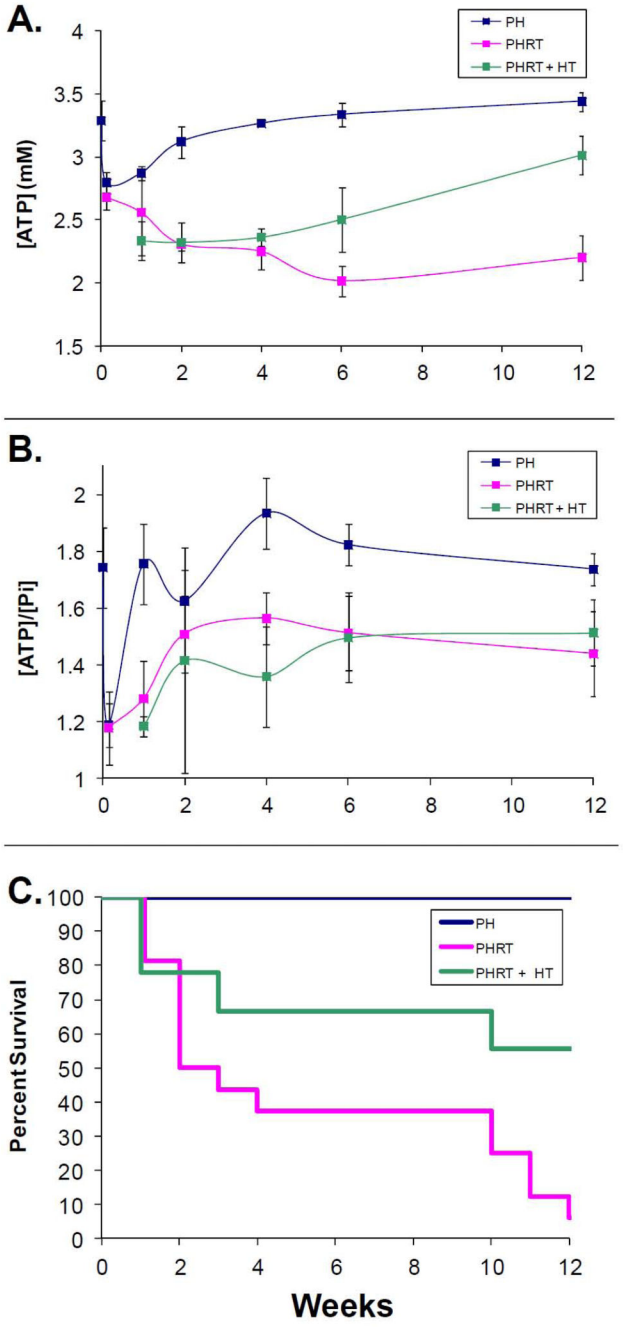

Figure 3.

a) Time courses for estimated [γ-ATP] for each group. The [γ-ATP] in the PHRT group remains depressed throughout the study. In contrast, [γ-ATP] returns to normal following PH alone within two weeks after PH. [γ-ATP] also gradually increases over time in the PHRT+HT group. However, the increase is gradual and approaches normal 12 weeks after PHRT+HT (3.0±0.12 mM). b) Time courses for the ratio of ATP/Pi signal are shown. Neither the PHRT nor the PHRT+HT groups return to control ATP/Pi values (1.74±0.05, PH) at 12 weeks (1.51±0.1 vs. 1.44±0.15, for PHRT+HT and PHRT respectively). c)

Kaplan-Meier survival curves for the three groups. Improved survival is seen in rats with hepatocyte transplant compared to those without ($p<0.005$).

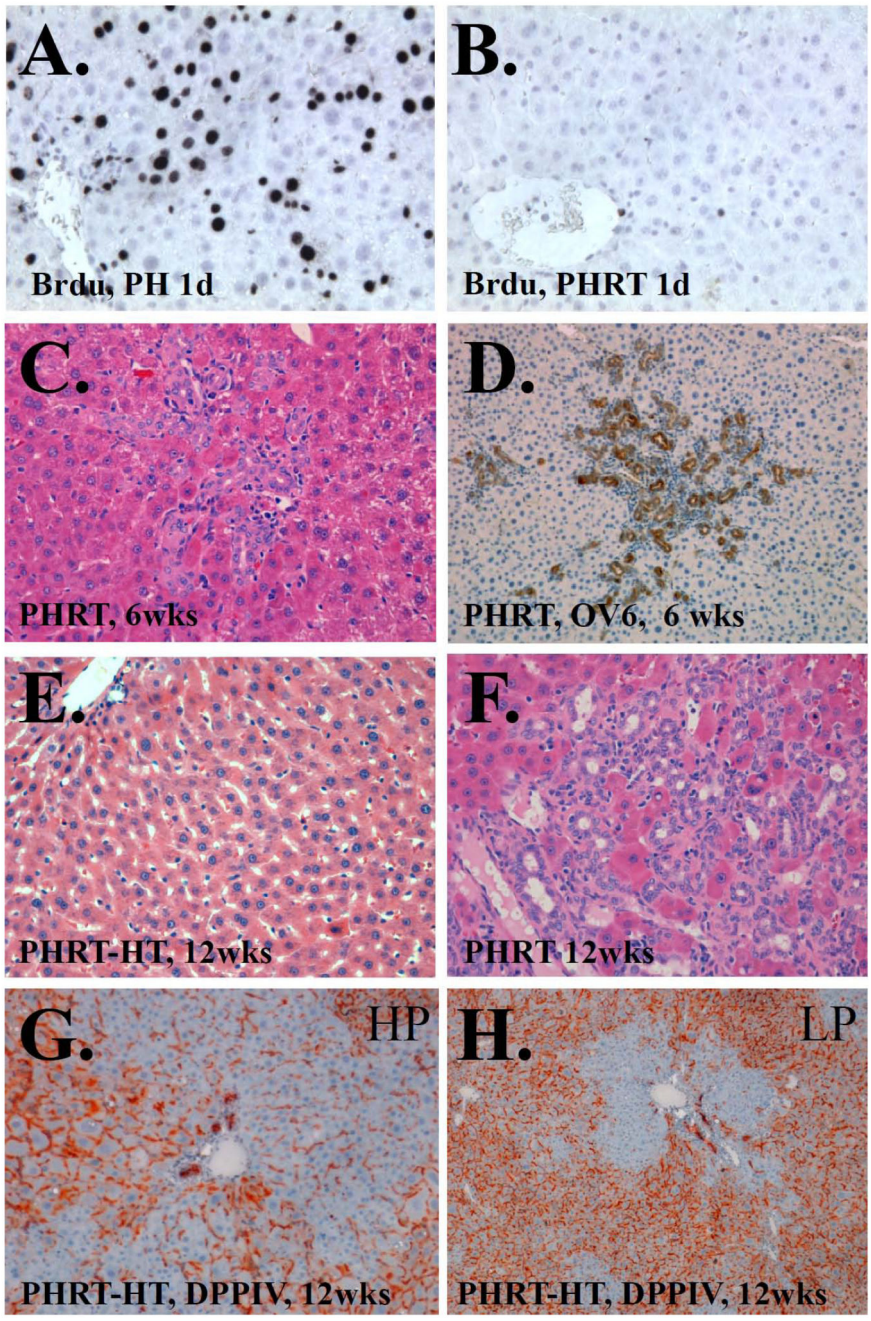

Figure 4.

BrdU immunohistochemistry following a) PH only or b) PHRT. BrdU incorpaoration is dramatically reduced by RT. c) H&E staining of rat liver 6 weeks after PHRT. Extensive bile ductular proliferation is seen. d) OV-6 immunhistochemistry of rat liver 6 weeks after PHRT confirms ductular and oval cell proliferation. e) H&E staining of rat liver 12 weeks after PHRT+HT. Normal appearing liver parychema is seen. f) In contrast, H&E staining of rat liver 12 weeks after PHRT shows pervenular collapse, pleomorphic nuclei, and extensive bile ductular reaction. g) High power view of DPPIV enzyme histochemist of PHRT +HT

rat liver at 12 weeks. DPPIV negative hepatocytes (blue) are seen proliferating in DPPIV positive (orange) parynchyma. h) Low power view indicates approximately 40% repopulation by transplanted hepatocytes.